

# Effect of Exhaust Gas Dilution Rate on Formation of Flameless Combustion of Liquid Fuel

Chun Loon Cha<sup>1</sup>, Ho Yeon Lee<sup>1</sup>, Pil Hyong Lee<sup>1</sup>, Sang Soon Hwang<sup>1\*</sup>

<sup>1</sup>Division of Mechanical System Engineering, Incheon National University, Incheon, South Korea 406-772

## Abstract

The effects of exhaust gas dilution rate on formation of flameless combustion with liquid fuel were analyzed using three-dimensional numerical simulations for application of gas turbine combustor with high thermal intensity. Results show that the spray model tends to overestimate spray penetration length a little bit at the beginning of the spray but the spray model acts well to predict the spray pattern and penetration length in general. Also the high temperature region was more localized and flame temperature was spatially uniformly distributed under condition of higher dilution rate of burnt gas similar as gas phase flameless combustion. And the average temperature was found to be reduced about 1000K at the higher dilution rate. The evaporation and mixing process of liquid fuel were found to be another important factor for formation of flameless combustion compared to gas flameless combustion.

## Introduction

Since the protocol of Kyoto was signed as an agreement for reducing greenhouse gases in 1997, the consciousness of the negative effect by combustion products such as a CO, NO<sub>x</sub> and unburned hydro carbon on human health has become to the fore as a big issue in the use of fossil fuels at combustion systems. Thus, many combustion techniques have been investigated in the past to achieve low pollutants emission for gas turbine combustors. Some examples include rich burn-quick quench-lean burn (RQL), catalytic combustion, lean direct injection, and ultra lean premixed combustion. But despite of the low pollutants emission characteristics depending on the operation in the region of lean flammable limit, these combustion technologies have shown high combustion instability phenomena inherently. [1]

“Flameless” combustion is considered as one the promising combustion technology for reducing NO<sub>x</sub> and CO emissions with improving thermal efficiency of combustion system. Flameless combustion was formed from the combination of theoretical and practical improvements such as the use of highly preheated air and exhaust gas recirculation. In the case of flameless combustion, instabilities can be prevented because of no existence of flame front. Indeed, when the turbulence is very high and the oxidizer temperature is above the auto-ignition temperature of the fuel (typically higher than 800°C), the flame is initiated in many locations simultaneously and randomly, making no single region of the flame dependent upon any other region. [2-5]

In flameless combustion, dilution of oxygen plays a very important role. An oxygen concentration of around 5% in molar fraction is mandatory to prevent flame formation. 5% is very low when compared with conventional combustion which is carried out with 21% (mol) oxygen. A method to satisfy the appropriate oxygen concentration necessary for flameless combustion is using internal recirculation, where air and fuel jets in a confined space can entrain combustion products from surroundings. [6] In order to quantify the

recirculation that exists in a confined system, Wunning and Wunning [7] defined a parameter known as the recirculation ratio ( $K_v$ ), which is the ratio between the gas mass flows entrained by all jets ( $\dot{m}_r$ ), and the sum of air ( $\dot{m}_a$ ) and fuel mass flows ( $\dot{m}_f$ ) in the discharge.

$$K_v = \frac{\dot{m}_r}{\dot{m}_f + \dot{m}_a} \quad (1)$$

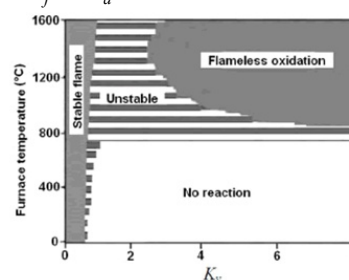


Fig.1. Schematic of flameless combustion stability limits.

Figure 1 shows the different combustion regime depending on recirculation ratio and furnace temperature. To obtain the flameless combustion regime it is necessary to have a recirculation ratio higher than 3 and a furnace temperature over the auto-ignition temperature (800°C). On the order side, flameless can be understood by study of the Damkohler Number ( $Da$ ) for the case of a well-stirred reactor.

$$D_a = \frac{\tau_{flow}}{\tau_{chem}}, \quad \tau_{flow} = \frac{L_T}{u'}, \quad \tau_{chem} = \frac{\delta_L}{S_L} \quad (2)$$

$$D_a = \left( \frac{L_T}{\delta_L} \right) \left( \frac{S_L}{u'} \right)$$

The reaction time is then large enough compared to the dissipation time of large eddies and yields the turbulence mixing to diffuse both the chemical and momentum gradients. Associated with sufficient preheated air, stable combustion domain can be reached even for high ratio of exhaust gas recycling.

\* Corresponding author: [hwang@incheon.ac.kr](mailto:hwang@incheon.ac.kr)

Figure 2 shows the flameless combustion region depending on the reaction time and the dissipation time of large eddies. According to this diagram, flameless combustion region is between the broken reaction zones and the thin reaction zones. The reduction of oxygen concentration and the high proportion of product gas (H<sub>2</sub>O, CO<sub>2</sub>) by the high recirculation make the broken reaction zone. The dilution of the fuel with the exhaust gases to minimize the concentration of oxygen before the mixing with fuel and air is the key role of formation of flameless combustion. Most flameless combustion has been focused on gas phase flameless combustion.

Our study will focus on the effects of exhaust gas dilution rate on formation of flameless combustion with liquid fuel used in almost gas turbine. Three-dimensional numerical simulations were adopted to analyze the combustion characteristics for application of gas turbine combustor with high thermal intensity. The kerosene was used to liquid fuel in this simulation. In the first part of this investigation, an experimental spray penetration length data measured by the EHPC (Eindhoven high pressure cell) and the Sandia National Laboratories were compared with calculated penetration length to verify the accuracy of liquid spray model in Fluent. In addition, temperature profile was also compared to analyze the effect of exhaust gas dilution rate on formation of flameless combustion.

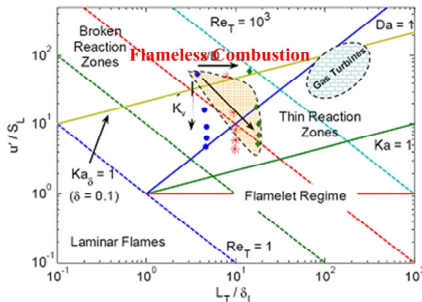


Fig.2. Borghi diagram of turbulent premixed combustion.

## 2. Numerical Models

### 2.1 Governing Equations

Mass conservation, momentum conservation, energy conservation, species conservation and discrete phase model (DPM) equations for reactive fluid flow are as follows:

#### 2.1.1 Mass conservation equation

$$\nabla \cdot (\rho \vec{v}) = S_m \quad (1)$$

#### 2.1.2 Momentum conservation equation

$$\nabla \cdot (\rho \vec{v} \vec{v}) = -\vec{\nabla} p + \rho \vec{g} + \vec{F} \quad (2)$$

#### 2.1.3 Energy conservation equation

$$\nabla \cdot (\vec{v} (\rho E + p)) = -\nabla \cdot \left( \sum_j h_j J_j \right) + S_h \quad (3)$$

### 2.1.4 Species conservation equation

$$\frac{d m_i''}{d x} = m_i'' \quad (4)$$

### 2.1.5 Discrete phase model equation

$$m_p \frac{d u_p}{d t} = F_{drag} + F_{pressure} + F_{virtualmas} + F_{gravity} + F_{other} \quad (5)$$

## 2.2 Numerical Simulation Models

The numerical simulation model is based on Semi-Implicit Method for Pressure Linked Equation Consistent algorithm using segregated solver of Ansys Fluent. Figure 3 represents the configuration of mesh structure for flameless combustion chamber. The number of mesh was about 100,000 and consisted of hexahedral mesh. Boundary conditions were set to non-slip wall, constant mass flow rate at the inlet and constant pressure condition at the outlet respectively. Each composition of chemical species, which applied to calculate for the dilution rates were summarized in Table 1. In case of the dilution rate ( $\psi$ ) is '0', oxygen was only used as a oxidizer. The mass fraction of exhaust gases was calculated by Chemkin Pro code at equivalence ratio 1.

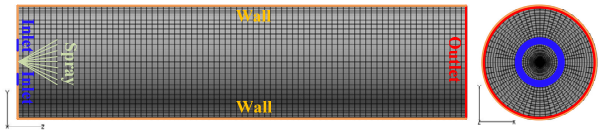


Fig.3. Mesh structure of computational domain.

Table 1 Mass fraction of components for each dilution rate

	Dilution rate ( $\psi$ )				
	0	0.3	0.5	0.7	0.9
O <sub>2</sub>	1.0	0.7	0.5	0.3	0.1
CO <sub>2</sub>	0	0.026	0.0435	0.061	0.078
H <sub>2</sub> O	0	0.056	0.0935	0.131	0.169
N <sub>2</sub>	0	0.218	0.363	0.508	0.653

## 3. Results and Discussions

### 3.1. Validation of the numerical spray model

To verify the accuracy of liquid spray model in Fluent, an experimental spray penetration length data measured by the EHPC (Eindhoven high pressure cell) and the Sandia National Laboratories were compared with calculated penetration length. Figure 4 shows the spray pattern of the liquid droplet at the 0.2ms time step. The shape of spray pattern was well predicted as set by 60° angle solid cone spray.



Fig.4. Predicted spray pattern of numerical spray model (t=0.2ms).

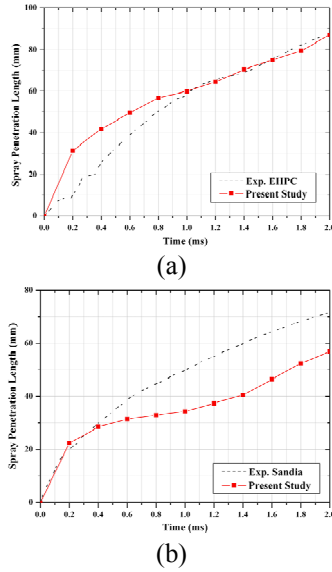


Fig.5. Compare the spray penetration length with numerical results and experimental results.

Moreover, two cases of experimental spray data were compared to each numerical data in Figure 5. The spray model tends to overestimate spray penetration length a little bit at the beginning of the spray but the spray model acts well to predict the spray pattern accurately after 1ms in figure 5(a) EHPC case. In figure 5(b) Sandia case, the spray model predicts well at the beginning of spray but underestimate after 0.4ms. Although it is not able to predict perfectly at all conditions, this spray model was expected to act well in our condition.

### 3.2. Effect of exhaust gas dilution rate on formation of flameless combustion

Figure 6 represents the contour of temperature for different dilution rate. Due to the influence of the oxy-fuel combustion, the calculated maximum temperature was very high up to 5000K. Also, the low temperature region was formed by the evaporation of kerosene and the low temperature of supplied gases.

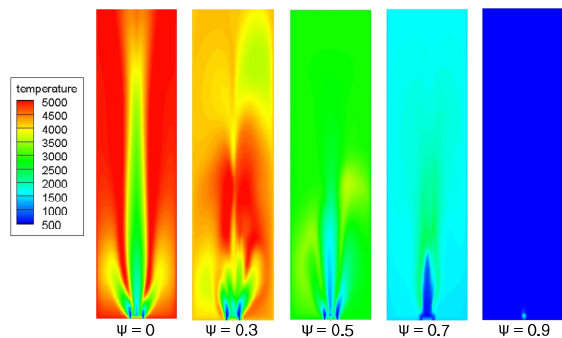


Fig.6. Contour of temperature for different dilution rate.

In order to analyze more detail of the temperature distribution, the temperature of the center line along the axial direction was shown in Figure 7. The local high temperature region was decreased and flame temperature was spatially uniformly distributed due to

higher dilution rate of burnt gas as similar pattern of gas phase flameless combustion. Therefore, the average temperature was reduced about 1000K as the increasing of dilution rate. It is also observed that the evaporation and mixing process of liquid fuel were found to be another important factor for formation of flameless combustion.

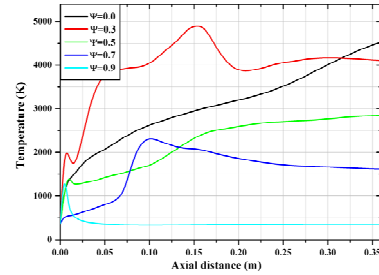


Fig.7. Temperature distribution along the axial distance for different dilution rate.

### 4. Conclusions

Liquid fuel flameless combustion was characterized numerically by using a Ansys Fluent commercial simulation code. The following results of this work could be useful for understanding the role of burnt gas recirculation to the formation of flameless combustion.

- 1) To validate prediction accuracy of spray model, it was compared with the experimental results which are from EHPC and Sandia. Although it is not able to predict perfectly at all conditions, it is confirmed that this spray model will act well in our condition.
- 2) To analyze the effect of exhaust gas dilution rate on formation of flameless combustion, the temperature distribution was investigated. The high temperature region was more localized and flame temperature was spatially uniformly distributed due to higher dilution rate of burnt gas as similar pattern of gas phase flameless combustion.
- 3) According to these results, the 50% to 70% amount of burnt gas recirculation was necessary for forming a flameless combustion. We also found that the evaporation and mixing process of liquid fuel were found to be another important factor for formation of flameless combustion.

### Acknowledgements

“This research was supported by Basic Science Research Program through the National Research Foundation of Korea (NRF) funded by the Ministry of Education” (No. 2013R1A1A2008833)

### Reference

- [1] A. Lacarelle, S. Goke, C.O. Paschereit, Proceedings of ASME Turbo Expo (2010) GT2010-23132.

[2] Erwann Guillou, Michael Cornwell, Ephraim Gutmark, AIAA 2009-225.

[3] A.M. Annaswamy, M. Fleifil, J.P. Hathout, and A.F. Ghoniem, Combustion Science and Technology vol.128 (1997) 131-180.

[4] M. Fleifil, J.P. Hathout, A.M. Annaswamy, and A.F. Ghoniem, Combustion Science and Technology, vol.133 (1998) 227-265.

[5] K. Ogata, Modern Control Engineering third edition (1997) Englewood Cliffs.

[6] Camilo Lezcano, Andres Amell, Francisco Cadavid, DYNA Vol.80 (2013) No.180.

[7] J. A. Wüning and J. G. Wüning, Progress in Energy and Combustion Science Vol. 23 (1997) No. 1 81-94.

[8] Weber, Roman, smart, John P., Kamp, Willem vd, Proceedings of the Combustion Institute 30 (2005) 2623-2629.

[9] Pin-Chia Chen, Wei-Cheng Wang, William L. Roberts, Tiegang Fang, Fuel 103 (2013) 850-861.